ELSEVIER

Journal of Marine Systems 37 (2002) 3–15

JOURNAL OF MARINE SYSTEMS

www.elsevier.com/locate/jmarsys

Geostationary satellites reveal motions of ocean surface fronts

Richard Legeckis*, Christopher W. Brown, Paul S. Chang

National Environmental Satellite Data and Information Service, National Oceanic and Atmospheric Administration, 1315 East West Highway E/RA-31, SSMC3, Rm. 3620, Silver Spring, MD 20910 3282, USA

Received 27 December 2000; received in revised form 9 October 2001; accepted 8 April 2002

Abstract

A new method of locating and viewing ocean surface fronts is demonstrated in animations of daily composites of hourly sea surface temperatures derived from the NOAA Geostationary Operational Environmental Satellites (GOES). The animation of the satellite images allows the human eye to separate the faster-moving residual clouds from slower-moving ocean currents, fronts and eddies. The animations produce the sense of an ocean in motion that is not apparent in individual satellite images. Three years of GOES animations of sea surface temperatures of the Atlantic and Pacific Oceans are used to illustrate the westward propagation of Pacific Tropical Instability Waves (TIW) during La Niña, the seaward deflection of the Gulf Stream at the Charleston Bump, a time series of the Loop Current and separation of six warm core eddies in the Gulf of Mexico, and the cyclonic eddies and westward-moving meridional fronts near the Hawaiian Islands.

Keywords: Ocean surface fronts; GOES; Sea surface temperatures

1. Introduction

Ocean surface fronts have been studied extensively with a variety of satellite sensors and direct observations (Ullman and Cornillon, 1999; Hickox et al., 2000). These fronts are often the boundaries of different water masses and can be recognized by sharp gradients of salinity, temperature and water color. Until recently, most of the satellite observations of ocean fronts have been made from polar orbiting satellites which view the same area of the earth once (visible) or twice (infrared) each day. These include observations of ocean color from the visible spectral bands of sensors such as SeaWiFS and surface ocean temperatures from thermal infrared bands of sensors such as AVHRR, ATSR and MODIS. In addition, ocean surface topography and geostrophic currents are estimated from microwave spectral bands of altimeters, such as on TOPEX/POSEIDON and Earth Resources Satellites (ERS).

The visible and infrared polar orbiting satellite measurements offer the highest spatial resolution (1 km) and provide detailed instantaneous views of ocean fronts. However, these satellite views are limited to cloud-free regions of the ocean twice each day. Typically, weekly or monthly composites are required to accumulate sufficient cloud-free observations to allow the generation of statistics associated with surface ocean fronts. However, since ocean

* Corresponding author. Tel.: +1-301-713-9384x111; fax: +1-301-713-4598.

E-mail address: Richard.Legeckis@noaa.gov (R. Legeckis).

0924-7963/02/$ - see front matter © 2002 Elsevier Science B.V. All rights reserved.
PII: S0924-7963(02)00192-6

fronts can move a considerable distance in several days, continuity is compromised. This lack of continuity of polar satellite observations limits the ability of oceanographers to monitor the evolution of ocean SST patterns.

The Geostationary Operational Environmental Satellites (GOES) can be used to improve the temporal observations of the oceans (Maul and Baig, 1975; Legeckis and Zhu, 1997). The most recent series of GOES (Menzel and Purdom, 1994) provides visible and infrared (3.9, 11 and 12 μ) images of the same area of the ocean every 30 min with a spatial resolution of 1 and 4 km, respectively at nadir. The GOES has been used extensively by meteorologists to monitor atmospheric fronts, clouds and weather patterns. The main attribute of GOES is the high frequency of daily observations from a fixed position above the earth. The rapid motion of intermittent clouds allows the accumulation of the cloud-free ocean areas during 1 day. However, the coarse spatial resolution limits the detection of SST patterns to length scales greater than 5 km.

To evaluate the GOES for ocean observations, 3 years of hourly GOES infrared imagery were obtained in the Atlantic and Pacific Oceans in the area shown in Fig. 1. Hourly SST images and daily SST composites were created and mapped at a spatial resolution of about 4 km at nadir. These daily composite images were viewed in rapid animation sequences. The human eye acts as a frequency discriminator between the relatively slowly moving ocean surface thermal patterns, the higher-frequency residual clouds and the random instrument infrared noise. The results reveal an unexpectedly complex "ocean in motion" and illustrate the time-dependent and often nonlinear nature of ocean surface interactions. Some of the SST animations can be seen at reduced spatial and spectral resolutions at: http://www.goes.noaa.gov (Select SST Animations).

2. SST images and animation method

The two NOAA GOES satellites are positioned above the equator at longitudes 75W and 135W in Fig. 1 and offer a view of large areas of both the Atlantic and the Pacific Oceans. The hourly SST images are created by applying a linear version of a SST algorithm (Wu et al., 1999; May and Osterman, 1998) which uses the 11 and 12 μ infrared channels to estimate an atmospheric correction. It is not possible to use a more accurate higher order equation because hot spots are produced along cloud edges in each image and daily composites are corrupted with exces-

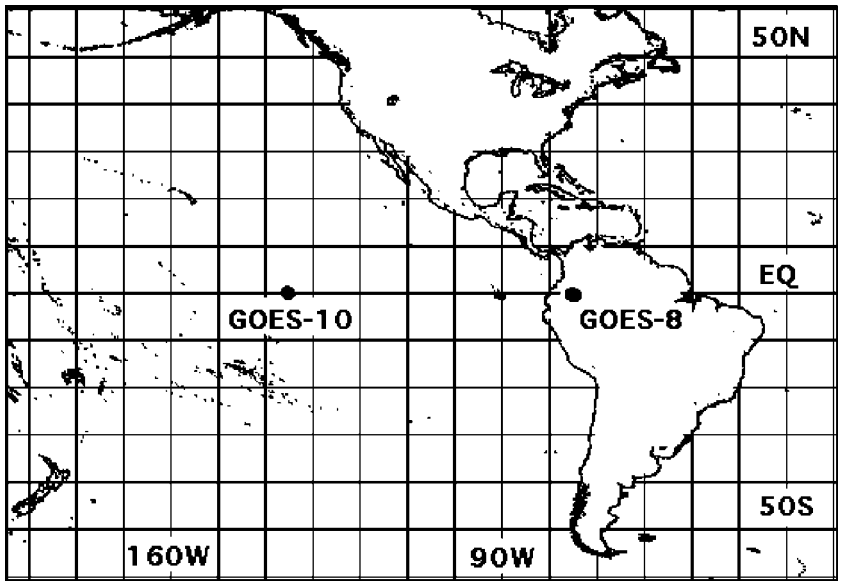

Fig. 1. The ocean area monitored by the two GOES satellites at the equator and longitudes 75W and 135W.

sive speckled noise patterns. The SST images are mapped to a rectilinear earth grid with equal spacing of 25 samples per degree (4.44 km/pixel at the equator).

After the SST image is created, it is converted to an 8-bit image to reduce data volume using the formula $SST = -10 + 0.2x$, where x equals 0–255 and SST are between −10 and 41 °C. The larger than required SST range (51 °C) for the 8-bit images is a trade-off for animations to allow detection of SST (−2 to 32 °C), low level clouds (−10 to 10 °C) and intermittent hot spots (28 to 40 °C) observed seasonally over the ocean. These hot spots are still under investigation but appear to be associated with low wind events and rapidly changing patterns of excessive atmospheric moisture.

Daily SST composites are created by retaining the warmest samples in each image. This procedure tends to remove the colder clouds that are moving over a warmer ocean surface. The composite interval can be increased to remove additional clouds or decreased to allow detection of diurnal heating in relatively cloud-free ocean areas (Legeckis and Zhu, 1997). Since the daily SST composite accumulates the warmer water associated with diurnal SST cycles, a bias of more than 1 °C can be introduced in some ocean areas. Seasonal heating produces isothermal surface conditions, which prevent the detection of current boundaries. However, in some cases, it was possible to use 8-day composites of ocean color (chlorophyll maxima) from the SeaWiFS (McClain et al., 1998) to establish the position of ocean fronts.

The composite image sequences are viewed rapidly on a Power Macintosh G4 using software provide by the National Institutes of Health (NIH). This combination of hardware and software provides optimum control and display capacity for viewing the long time series of GOES SST images. An animation rate of 5–15 days/s is required to produce an ocean in motion. All NIH software operations are carried out in computer memory so that animation sequences are limited by the available memory and the size and number of images. For example, the GOES East daily composite data set (1800 × 1500 pixels) extends from 111W to 39W and 55N to 5S and requires 2.7 Mb/image or nearly 1 Gb of memory for a year of daily composites.

The SST composite method has some limitations. For example, the spatial resolution of the GOES is degraded away from nadir due to earth curvature and

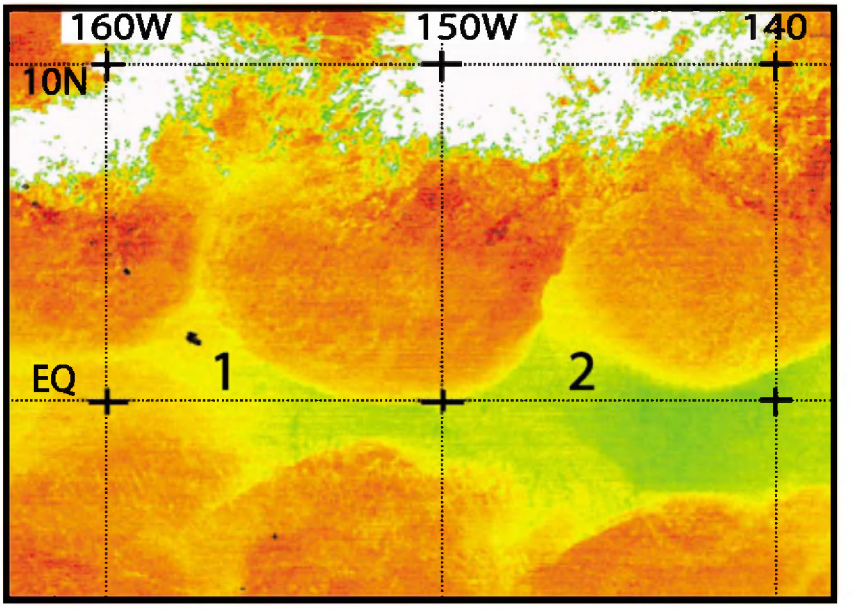

Fig. 2. The daily GOES SST composite of the equatorial fronts on September 3, 1998, Julian day 246. Two (1, 2) tropical instability wave crests appear north of the equator as well as a large (500 km) gyre centered at 3N and 143W.

there are many ocean areas with persistent cloud cover. The noise associated with the two adjacent detectors used for each GOES infrared channel introduces random SST uncertainty from 0.1 to 0.5 °C that obscures weak SST gradients. In the future, it may be possible to create digital filters to separate the ocean SST patterns and cloud patterns but instrument noise and low spatial resolution is presently a limiting factor.

3. GOES SST animations—the ocean in motion

The following description of selected ocean fronts between the years of 1998 and 2001 is intended to provide an overview of some of the dynamic events that can be observed in the GOES SST animations. The intent here is to inform the ocean community of this new geosynchronous perspective and to demonstrate that it is possible to obtain unique information about ocean surface events using animation.

In general, the SST patterns observed in the animations are associated with SST fronts that form due to coastal and equatorial upwelling or at the boundaries of currents such as the Gulf Stream, the Loop Current in the Gulf of Mexico and the Pacific South Equatorial Current. The following examples will illustrate some of the information that can be extracted from the GOES SST animations:

- Tropical Instability Waves (TIW) and equatorial upwelling during La Niña
- Seaward deflection of the Gulf Stream off Charleston, SC

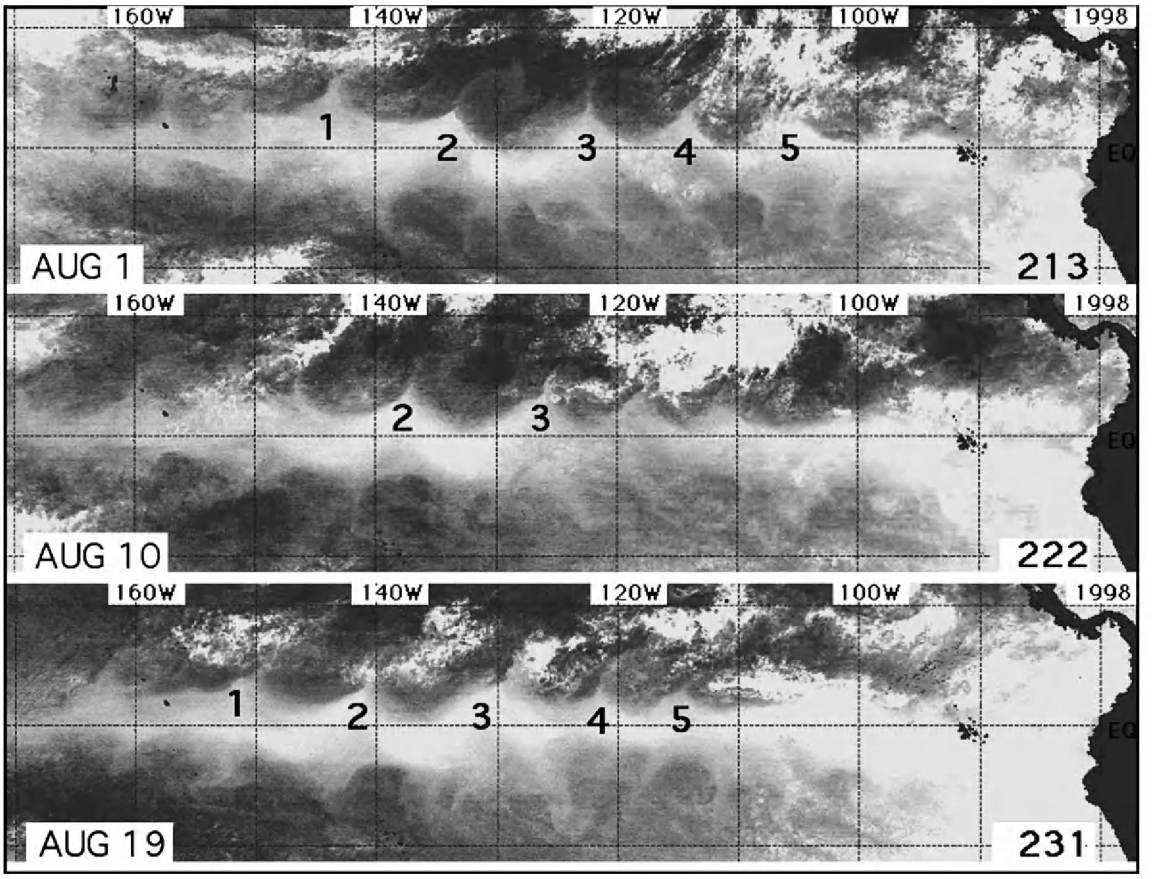

Fig. 3. Three daily GOES SST composites in the equatorial Pacific during the La Niña of 1998 on Julian days 213, 222 and 231. The westward propagation of the wave crests (1–5) is evident. Darker shades are warmer water.

- Separation of eddies from the Loop Current in the Gulf of Mexico
- Eddies and fronts near the Hawaiian Islands.

4. Tropical Instability Waves (TIW) and La Niña

The most dramatic event recorded by the GOES SST animations is the return of the equatorial Pacific cooling and the westward-moving Tropical Instability Waves (TIW) associated with La Niña in 1998 and 1999, after the El Niño of 1997 (Delcroix et al., 2000; McPhaden, 1999). The equatorial long wave patterns near the equator are instabilities (Philander et al., 1985; Legeckis, 1977) introduced by the shear of the westward-flowing SEC and the eastward-flowing North Equatorial Counter-Current (NECC). Model studies at Princeton University (Cox, 1980) predict a nominal TIW period of 30 days and wavelength of 1000 km.

The TIW SST fronts north of the equator have sharp peaks and long troughs as illustrated on September 3, 1998 (day 246), between longitudes 140W and 165W in Fig. 2. A sequence of daily SST composites during 1998 show the wave positions on August 1, 10 and 19 (days 213, 222 and 231) in Fig. 3 and the westward phase velocity of seven of the most distinct wave crests is shown in Fig. 4. The average wave speed is estimated in Table 1 for the duration of each wave crest and the wave period is estimated at each longitude from the number of days between two successive wave crests at that longitude. The average speed and period are used to compute the wavelengths in Table 2.

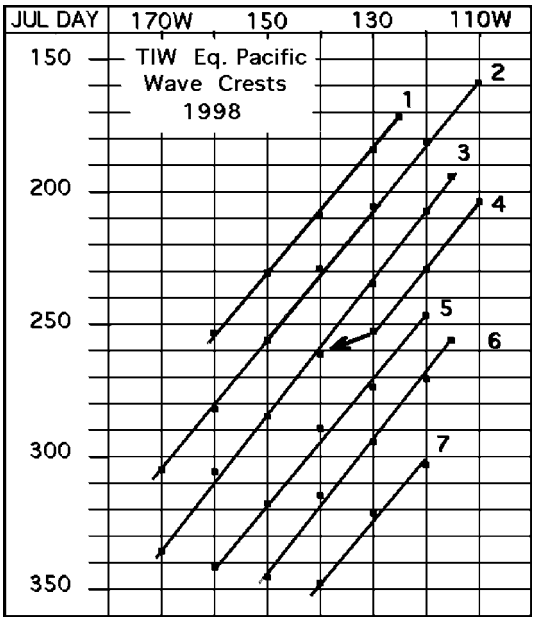

Fig. 4. The positions of the main wave crests (1–7) in the equatorial Pacific during 1998. The fourth wave crest appears to merge rapidly with the third wave crest near longitude 135W.

Table 1
Tropical Instability Waves (TIW)—period and speed

1998	110W	120W	130W	140W	150W	160W	170W	Speed
1			23	23	26	29		47.6
2	22	27	29	32	29	25	30	45.3
3	23	21	17	33	32	35		43.3
4	16	18	21					46.3
5	26	23	23	26	28			47.2
6		31	26	30				43.4
7								49.3

The period and average speed of Pacific TIW during 1998.

The fourth and third wave crest appeared to merge rapidly after day 245 at longitude 135W in Fig. 4. It is of interest to note that a similar interaction occurred at the same location during the La Niña of 1983 after November 16 (day 320) (Legeckis, 1984: Fig. 3 wave phase for 1983). This may indicate wave–wave interactions that become noticeable due to the continuity of the animations. Clockwise-rotating vortices can sometimes be detected north of the SST wave front and to the east of a wave crest as in Fig. 2 at longitude 143W. These vortices have radii of about 500 km and move westward along with the wave fronts.

The TIW move westward until March of 1999 and subsequently became disorganized during the seasonal warming of equatorial waters. From April to mid-June,

Table 2
Tropical Instability Waves (TIW)—wavelength

1998	110W	120W	130W	140W	150W	160W	170W
1			1090	1090	1240	1380	
2	1000	1220	1310	1450	1310	1360	1360
3	1000	910	740	1430	1390	1520	
4	740	830	970				
5	1230	1090	1090	1230	1320		
6		1350	1130	1300			

The wavelengths of Pacific TIW during 1998.

there is a weak eastward drift of SST patterns at the equator between latitudes 170W and 130W. Westward of South America, the TIW reappear in June of 1999 and start their formation and westward propagation from the vicinity of the Galapagos Islands.

The TIW are observed each year in satellite SST images except during El Niño events when equatorial SST fronts become weak or disappear. Based on polar orbiting satellite SST time series since 1982, the most intense TIW occur the year following an El Niño event. Especially intense TIW are observed after the month of May during 1983, 1988 and 1998, the year following the major El Niño events. The monitoring of the equatorial SST patterns with GOES animations provides a clue to the onset, duration and evolution of La Niña.

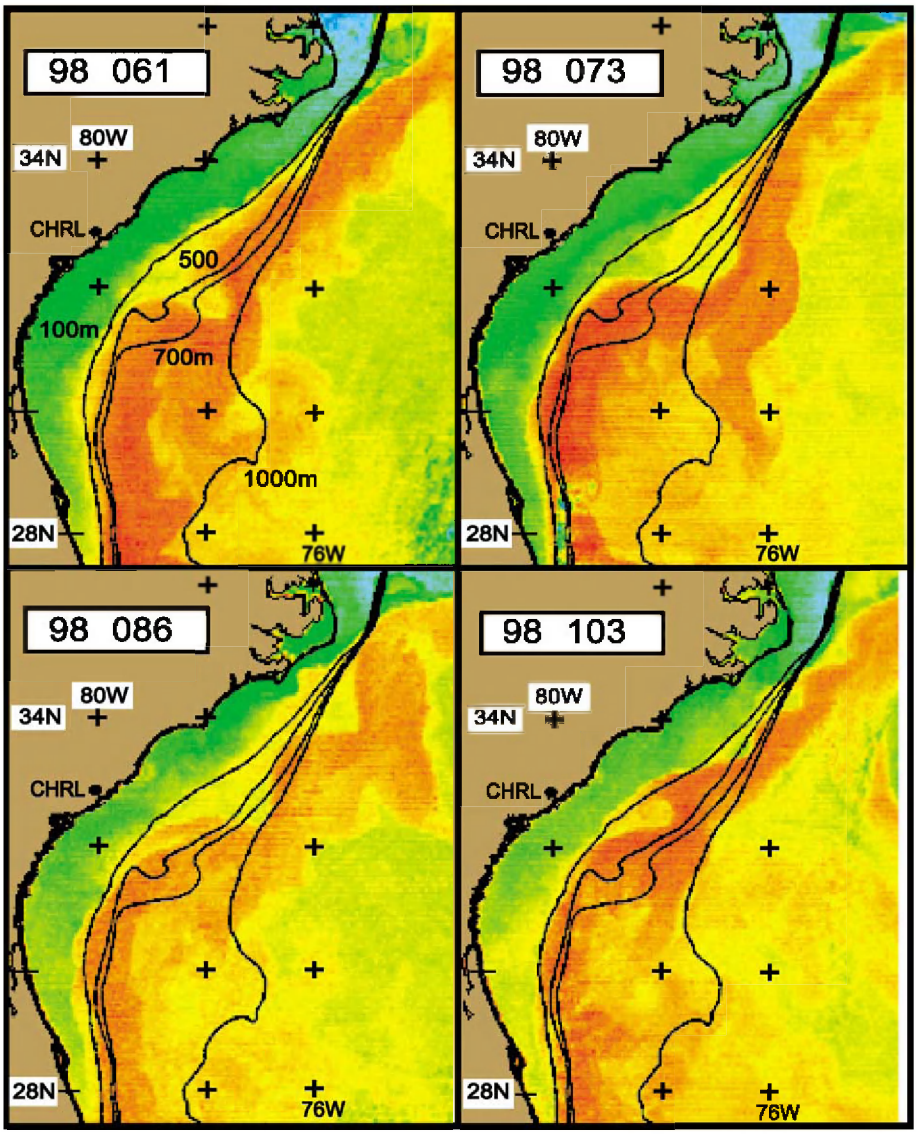

Fig. 5. Four daily GOES SST composites of the time-dependent seaward deflection of the Gulf Stream at the Charleston Bump, located about 100 km southeast of Charleston, SC (CHRL).

5. Deflection of the Gulf Stream off Charleston, South Carolina

The Gulf Stream flows through the Florida Straits and follows the nearly parallel bottom contours of the continental shelf until Charleston, SC. The Charleston Bump refers to a mound-like elevation in ocean bottom topography which is located approximately 100 km southeast of Charleston (Popenoe and Manheim, 2001). The Gulf Stream is often deflected seaward at the Bump as shown during 1998 in Fig. 5. The persistent counterclockwise rotation of the Gulf Stream at the Bump is referred to as the Charleston Gyre and can be observed often in satellite infrared images (Brooks and Bane, 1978; Legeckis, 1979; McClain et al., 1984).

The Gulf Stream deflection at the Charleston Bump is not steady and is punctuated by repeated transient events in the form of northward travelling waves along the western edge of the SST front. Downstream of the Bump, the entire Gulf Stream often appears to meander as a wave train. Orlanski and Cox (1973) predict the propagation of these baroclinic waves along the western edge of the Gulf

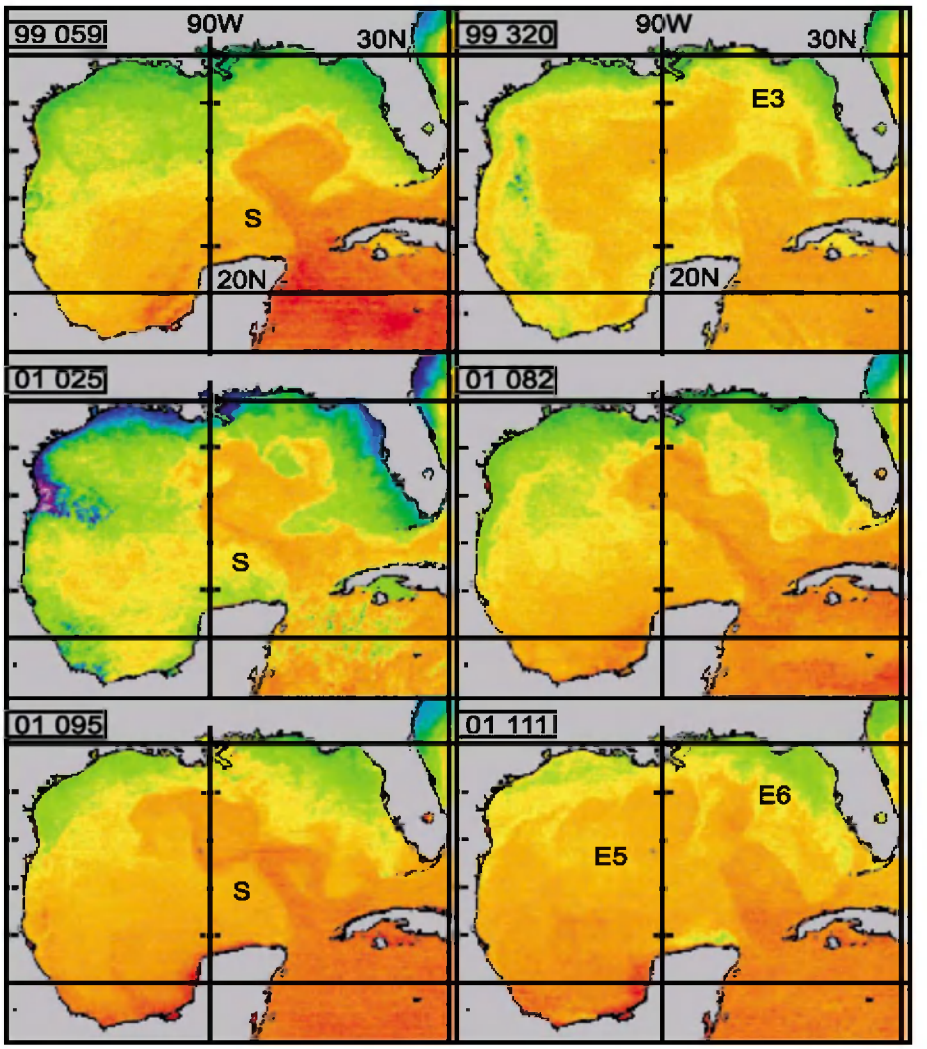

Fig. 6. Six daily SST composites of the Loop Current in the Gulf of Mexico before and after the separation (S) of warm core eddies (E).

Stream front. The baroclinic wave phase speed is opposite to the current but advection produces an apparent downstream propagation in the GOES animations that is considerably slower (50–100 cm/s) than the peak speed of the Gulf Stream (200 cm/s).

The western edge of the Gulf Stream is also marked by small-diameter (10 km) cyclonic eddies (Lee and Mayer, 1977) that propagate downstream along the edge. These eddies produce upwelled water at their core and their cyclonic rotation transfers warmer Gulf Stream waters toward the shore. This leads to the formation of double SST fronts, called *shingles* (VonArx et al., 1955), at the western edge of the Gulf Stream.

Although it is not possible to detect these small eddies in the GOES animations, the shingles are evident and one can assume the presence of an eddy at their source. These small cyclonic eddies are important in the mixing and nutrient replenishment process at the edge of the Gulf Stream. During a 250 day interval from the fall of 1998 to the spring of 1999, it was possible to identify the advection of nearly 30 of these cyclonic eddies downstream of the Charleston Bump in the GOES animations.

6. Separation of the Loop Current in the Gulf of Mexico

The SST fronts in the Gulf of Mexico are dominated by the Loop Current which enters the Gulf through the Yucatan Strait and exits through the Straits of Florida (Murphy et al., 1999; Vukovich, 1995; Molinari et al., 1977). It is well known that the Loop can separate after extending northward into the Gulf. The resulting large warm core eddies tend to drift southwestward. The GOES SST animations reveal that the Loop can sometimes reabsorb these eddies and revert to a continuous Loop Current.

The GOES SST animations reveal only part of the Loop Current separation sequence since the SST fronts disappear from about days 150 to 300 of each year due to seasonal heating of surface waters as described earlier by Muller-Karger et al. (1991). However, it was possible to establish the continuity of Loop observations by two other methods. In the first case, 8-day composites of ocean color (chlorophyll maxima) images from the SeaWiFS (McClain et al., 1998) provided a clue to the position of the Loop Current during the gaps in the GOES data. In the second case, cool waters from upwelling along the coast of Yucatan, Mexico (88W and 22N), were entrained by the Loop during summer months and provided a pattern that sometimes outlined the position of the Loop. Six examples of daily SST composites of the Loop are shown in Fig. 6 between 1999 and 2001. The time series of the northern limit of the Loop is shown in Fig. 7. The Loop tends to move northward during the fall of each year and at least six separated eddies (E) were identified and their positions are summarized in Table 3. Initially, the warm core anticyclonic eddies tend to be elliptical. Note that the major axis of the elliptical eddy (E3) in Table 3 rotates 90° clockwise between

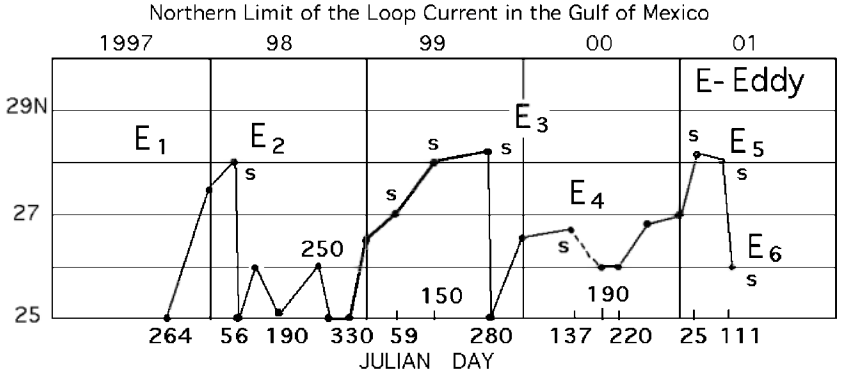

Fig. 7. The time series of the position of the northern limit of the Loop Current, the apparent separation (S) of eddies and six permanently separated eddies (E1–E6). The dashed lines indicate lack of verification data.

Table 3
Gulf of Mexico eddies—center and dimensions

Eddy	Longitude (W)	Latitude (N)	Year (day)	E–W (km)	N–S (km)
E1	91.5	26	98 (008)	220	260
E1	95.5	24	98 (168)	220	220
E2	87	26	98 (056)	380	280
E2	90	25	98 (168)	320	240
E3	89	26	99 (320)	500	300
E3	90	25.5	99 (365)	280	440
E4	87	26.5	00 (137)	380	250
E5	90	26	01 (100)	360	320
E6	87	27	01 (111)	160	220

The center positions and dimensions of warm core eddies (E) in the Gulf of Mexico shown in Fig. 7.

November 16 (day 320) and December 31 (day 365).

There were some occasions when the Loop appeared poised for separation (S) but eddies (E) did not persist as shown in Figs. 6 and 7. For example, the Loop appeared ready to separate in 1999 in Fig. 6 on February 28 (day 59) and again on May 30 (day 150) but a permanent eddy (E3) was not observed in SST images until October 7 (day 280). The absence of eddy separation is verified in 8-day composite images of surface chlorophyll from SeaWiFS between May 12 (day 132) and August 28 (day 240) in 1999. The two SeaWiFS images in Fig. 8 show the Loop Current as chlorophyll minimum. Likewise, the Loop appears ready for separation on January 25 of 2001 in Fig. 6 but does not separate into two eddies (E5 and E6) until after April 10 (day 100). Therefore, the GOES animations show that Loop can reabsorb eddies as suggested by Muller-Karger et al. (1991).

The GOES SST animations also reveal a persistent SST front each year along the western boundary of the Gulf of Mexico and it is assumed to be the edge of a western boundary current as suggested in earlier hydrographic data (Vidal et al., 1999) or the interaction of eddies with the continental margin as described by Biggs and Muller-Karger (1993). Northward-moving shelf waves are seen occasionally along the western boundary of the front, similar to those found along the edge of the Gulf Stream, south of Cape Hatteras. In addition, this front can often be seen during the summer, in spite of the seasonal surface heating.

7. Eddies and fronts near the Hawaiian Islands

The GOES SST animations reveal the temporal development and decay of cyclonic eddies and SST fronts in the vicinity of the Hawaiian Islands between 1998 and 2000. The meridional SST fronts, illustrated in Fig. 9, appear as bands of warmer water separated by 400–500 km and their westward displacements are summarized in Table 4. The speed and direction of these fronts appear to be similar to that reported earlier from low-frequency subsurface current meter measurements by Niiler and Hall (1988) at 28N and 152W.

Cyclonic eddies have been detected to the west of the Island of Hawaii. One of these eddies, with a diameter of about 50 km, appeared on February 2 (day

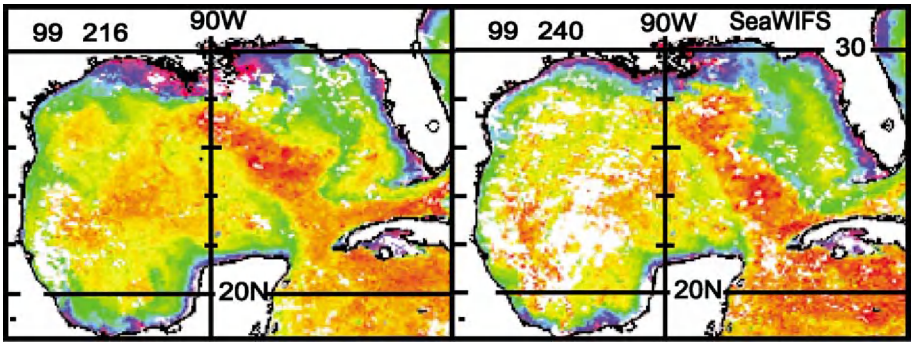

Fig. 8. Eight-day composites of surface chlorophyll maximum estimated from the SeaWiFS in the Gulf of Mexico on days 216 and 240 in 1999. The Loop Current has a chlorophyll minimum.

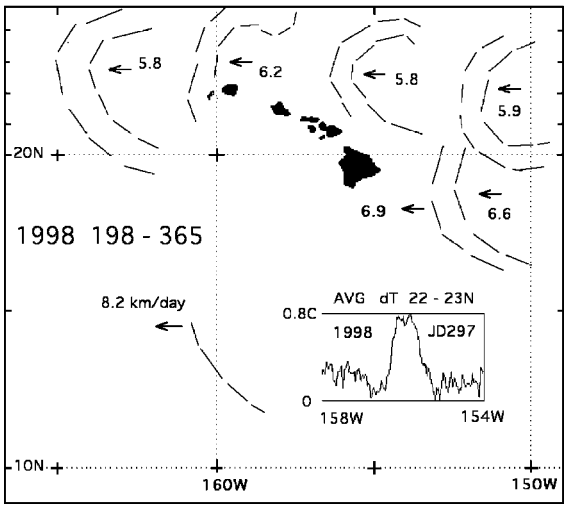

Fig. 9. The westward motion of SST fronts around Hawaii during 1998 from GOES SST composites. The typically weak SST change (0.8 °C) at the meridionally oriented front is shown on day 297.

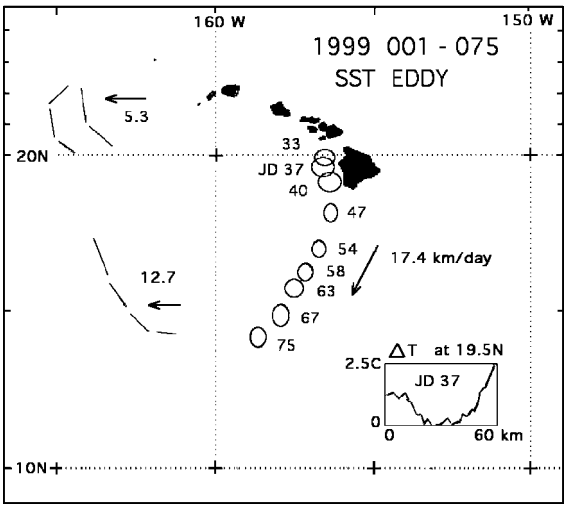

Fig. 10. The locations of a cyclonic eddy (days 33–75) and SST fronts which formed in the lee of the Island of Hawaii during February and March of 1999.

33) of 1999 as shown in Fig. 10. It moved to the southern tip of the big Island by February 13 (day 44), and then proceeded south to southwest for at least 500 km at an average speed of 17 km/day before disappearing from view due to loss of thermal contrast. The eddy displacement was only perceived by the use of the GOES SST animations and the eddy could not be easily detected in single SST images. The track of this eddy was also verified for a short interval in the 8-day SeaWiFS chlorophyll composites from February 2 to 25 (days 40, 48 and 56).

A cyclonic eddy appeared west of the Island of Hawaii on May 18 (day 138) of 1999 at 20N and 156.7W. The initial diameter of 50 km increased to 90 km by July 19 (day 200). Subsequently, the eddy became elliptical and the major axis rotated counterclockwise with a period of 15 days as shown in Fig. 11. This precession rate indicates low-frequency wave motion along the perimeter of the eddy, similar to that obtained for a cyclonic elliptical eddy south of the Gulf Stream (Spence and Legeckis, 1981). The 14-day composite of the boundaries of the precessing eddy is shown in Fig. 11. It is apparent that the dimensions of an eddy in a composite image can be distorted by precession and this must be considered when evaluating composites of a sequence of satellite images.

Between August 28 and December 2 (days 240 and 336) the eddy moved from its initial location to 20.5N

Table 4
Hawaii fronts—average westward speed

Fronts	Longitude (W)	Latitude (N)	Julian day start	Julian day end	Days	km	km/day	±
1998	150	18	259	298	39	260	6.6	0.7
	150	22	269	307	38	225	5.9	0.7
	153.5	23	241	272	31	180	5.8	0.8
	155.5	18	298	332	33	228	6.9	0.8
	156.5	23	238	268	30	186	6.2	0.8
	155.2	23	272	350	76	440	5.8	0.35
	160	23	298	348	50	290	5.8	0.5
	160	15	198	210	12	100	8.2	2.0
1999	160	15	1	33	32	210	12.7	0.8
	163.5	22	1	39	38	200	5.3	0.7

The starting positions and the average westward speed of the meridional SST fronts around Hawaii from mid-1998 to 1999.

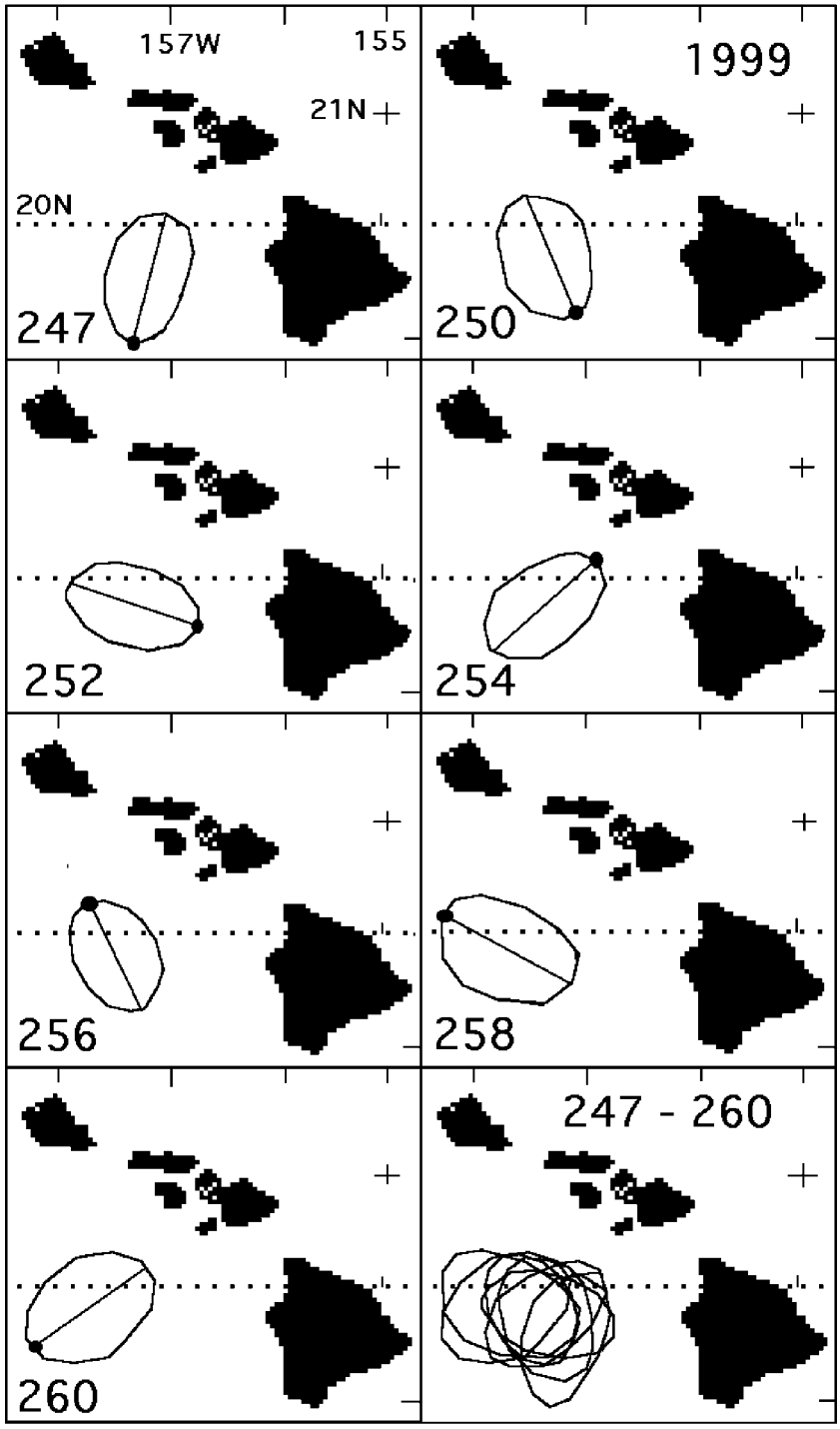

Fig. 11. The cyclonic elliptical cold core eddy, named Loretta, west of the Island of Hawaii between days 247 and 260 of 1999. The major axis rotated counterclockwise with an average period of 15 days.

and 160.8W at an average speed of 4 km/day. The SeaWiFS 8-day chlorophyll composites also revealed the eddy position from June 25 to December 2 (days 176–336). The chlorophyll signal appeared about 30 days after the appearance of cool waters at the cyclonic eddy. The SeaWiFS continued to reveal the eddy position after October 5 (day 278) while the GOES SST gradients disappeared. The biological enhancement and hydrography of this eddy, named *Loretta*, is described in detail by Seki et al. (2001) with in situ and satellite observations.

During 2000, a small eddy appeared on March 27 (day 86) and disappeared by April 14 (day 104). Subsequently, a large (100 km) elliptical eddy appeared on October 13 (day 286) and was still present on November 29 (day 332). The eddy maintained its position in the lee of the big Island but did appear to change shape significantly as it rotated. The NOAA Hawaii CoastWatch site tracks the cyclonic ocean eddies in the lee of Island of Hawaii with GOES SST and SeaWiFS composites and the cyclonic eddies are given unique names, similar to the way hurricanes are named by meteorologists.

8. Summary

The animation of the daily GOES SST composites provides the first opportunity to view the continuity of the daily motions of ocean surface thermal fronts not usually possible in imagery from polar orbiting sensors. If a picture is worth a thousand words, imagine what a thousand images provide when they are viewed rapidly. Animations provide a technique to convey and interpret a large amount of information quickly and easily. There are 8760 hourly GOES images in 1 year. Daily composites reduce this to 365 images, and the entire year can be viewed in less than 1 min at the rate of 10 frames per second. When time is compressed, the human eye can detect ocean variability that is usually hidden from view by intermittent cloud cover.

Although the composite animations reveal new information, the present GOES capability provides only a hint of what could be done with improved instrumentation. The present observational limitations are due to the coarse spatial resolution of GOES SST (about 4–8 km per sample in the field of view), the instrument noise and the seasonal hot spots in the GOES SST observations during summer months, both at the surface of the ocean and in the moist lower atmosphere. When the quality and spatial resolution of future geostationary satellites are improved, it will be possible to apply the SST composite technique to obtain an improved global view of the variability of ocean surface temperature fronts. The next generation of geostationary satellites (MSG) to be launched by EUMETSAT in 2002 will provide a view of the oceans at a resolution of 2 km while further improvements in geostationary satellites at NOAA are expected towards the end of this decade.

Acknowledgements

The GOES study of ocean fronts was supported by the NOAA Ocean Remote Sensing (NORS) project. The NIH animation software used in this project is free at: http://www.rsb.info.nih.gov/nih-image. Examples of composite SST animations are at: http://www.goes.noaa.gov Select: SST Animations. The new GOES SST cloud-cleared image products are distributed through anonymous FTP by NOAA Satellite Active Archive (SAA) at ftp://saasp1.saa.noaa.gov. The use of SeaWiFS data is in accordance with SeaWiFS Research Data Use Agreement. The NOAA CoastWatch satellite data and related sites are at: http://cwatchwc.ucsd.edu.

References

Biggs, D.C., Muller-Karger, F.E., 1993. Ship and satellite observations of chlorophyll stocks in warm- and cold-core rings in the western Gulf of Mexico. J. Geophys. Res. 99 (C4), 7371–7384.

Brooks, D., Bane, J., 1978. Gulf Stream deflection by a bottom feature off Charleston, South Carolina. Science 201, 1225–1226.

Cox, M., 1980. Generation and decay of 30 day waves in the numerical model of the Pacific. J. Phys. Oceanogr. 10, 11681–11686.

Delcroix, T., Dewitte, B., duPenhoat, Y., Masia, F., Picaut, J., 2000. Equatorial waves and warm pool displacements during the 1992–1998 El Niño Southern Oscillation events: observations and modeling. J. Geophys. Res. 105 (C11), 26045–26062.

Hickox, R., Belkin, I.M., Cornillon, P., Shan, Z., 2000. Climatology and seasonal variability of ocean fronts in the East China, Yellow and Bohai Seas from satellite SST data. Geophys. Res. Lett. 27 (18), 2945–2948.

Lee, T.N., Mayer, D.A., 1977. Low frequency current variability and spin-off eddies along the shelf off southeast Florida. J. Mar. Res. 35, 193–220.

Legeckis, R., 1977. Long waves in the eastern equatorial Pacific Ocean—a view from a Geostationary Satellite. Science 197 (4309), 1179–1181.

Legeckis, R.V., 1979. Satellite observations of the influence of bottom topography on the seaward deflection of the Gulf Stream off Charleston, South Carolina. J. Phys. Oceanogr. 9 (3), 483–497.

Legeckis, R., 1984. Monitoring of long waves in the Eastern Equatorial Pacific 1981–83 using satellite multi-channel sea surface temperature charts. NOAA Tech. Rep. NESDIS 8 (Washington, DC).

Legeckis, R., Zhu, T., 1997. Sea surface temperatures from the GOES-8 geostationary satellite. Bull. Am. Meteorol. Soc. 78 (9), 1971–1983.

Maul, G.A., Baig, S., 1975. A new technique for observing mid-latitude ocean currents from space. Papers in the 41st Annual Meeting, American Society of Photogrammetry, March 1–14, 1975, Falls Church, VA.

May, D.A., Osterman, W.O., 1998. Satellite-derived sea surface temperatures: evaluation of GOES-8 and GOES-9 multispectral image retrieval accuracy. J. Atmos. Ocean. Technol. 15, 788–797.

McClain, C.R., Pietrafesa, L.J., Yoder, J.A., 1984. Observations of Gulf Stream-induced and wind-driven upwelling in the Georgia Bight using ocean color and infrared imagery. J. Geophys. Res. 89 (C3), 3705–3723.

McClain, C.R., Cleave, M.L., Feldman, G.C., Gregg, W.W., Hooker, S.B., Kuring, N., 1998. Science quality of SeaWiFS data for global biosphere research. Sea Technol., 10–16 (September).

McPhaden, M.J., 1999. Genesis and evolution of the 1997–1998 El Niño. Science 283, 950–954.

Menzel, W.P., Purdom, J., 1994. Introducing GOES-I, 1994: the first of a new generation of geostationary operational environmental satellites. Bull. Am. Meteorol. Soc. 75, 757–781.

Molinari, R.L., Baig, S., Behringer, D.W., Maul, G.A., Legeckis, R., 1977. Winter intrusions of the loop current. Science 198, 505–507 (4 November).

Muller-Karger, F.E., Walsh, J.J., Evans, R.H., Meyers, M.B., 1991. On the seasonal phytoplankton concentrations and sea surface temperature cycles of the Gulf of Mexico as determined by satellites. J. Geophys. Res. 96 (C7), 12645–12665.

Murphy, S.J., Hurlburt, H.E., O'Brien, J.J., 1999. The connectivity of eddy variability in the Caribbean Sea, the Gulf of Mexico, and the Atlantic Ocean. J. Geophys. Res. 104 (C1), 1431–1453.

Niiler, P.P., Hall, M.M., 1988. Low frequency eddy variability at 28N and 152W in the Eastern North Pacific subtropical gyre. J. Phys. Oceanogr. 18, 1670–1685.

Orlanski, I., Cox, M.D., 1973. Baroclinic instability in ocean currents. Geophys. Fluid Dyn. (4), 297–332.

Philander, G., Halpern, D., Hansen, D., Legeckis, R., Miller, L., Paul, C., Watts, R., Weisberg, R., Wimbush, M., 1985. Long waves in the Equatorial Pacific. Trans.-Am. Geophys. Soc. 66 (14), 154 (2 April).

Popenoe, P., Manheim, F.T., 2001. Origin and history of the Charleston Bump—geological formations, currents, bottom conditions, and their relationship to wreckfish habitats on the Blake Plateau. In: Sedberry, G.R. (Ed.), Island in the Stream, Oceanography and Fisheries of the Charleston Bump. Am. Fish. Soc. Symposium 25, 28–29 Oct. 1999. American Fisheries Society, Bethesda, MD.

Seki, M.P., Polovina, J.J., Brainard, R.E., Bidigare, R.R., Leonard, C.L., Foley, D.G., 2001. Biological enhancement at cyclonic eddies tracked with GOES thermal imagery in Hawaiian waters. Geophys. Res. Lett. 28 (8), 1583–1586.

Spence, T.W., Legeckis, R., 1981. Satellite and hydrographic observations of low frequency motions associated with a cold core Gulf Stream Ring. J. Geophys. Res. 86 (C3), 1945–1953.

Ullman, D.S., Cornillon, P.C., 1999. Satellite-derived sea surface temperature fronts on the continental shelf off the northeast U.S. Coast. J. Geophys. Res. 104, 23459–23478.

Vidal, M.V.V., Vidal, F.V., Meza, E., Portilla, J., Zambrano, L., Jaimes, B., 1999. Ring–slope interactions and the formation of the western boundary current in the Gulf of Mexico. J. Geophys. Res. 104 (C9), 20523–20550.

VonArx, W.S., Bumpus, D.F., Richardson, W.S., 1955. On the fine structure of the Gulf Stream front. Deep-Sea Res. 3, 46–65.

Vukovich, F.M., 1995. An updated evaluation of the Loop Current's eddy shedding frequency. J. Geophys. Res. 100, 8655–8659.

Wu, X., Menzel, W.P., Wade, G.S., 1999. Estimation of sea surface temperatures using GOES-8/9 radiance measurements. Bull. Am. Meteorol. Soc. 80 (6), 1127–1138.